

## Charge-transfer and impact-ionization cross sections for fully and partially stripped positive ions colliding with atomic hydrogen\*

R. E. Olson and A. Salop

*Molecular Physics Center, Stanford Research Institute, Menlo Park, California 94025*

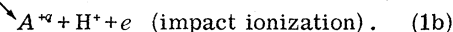
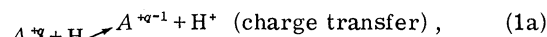
(Received 28 February 1977)

Classical trajectory calculations have been used to predict the charge-transfer and impact-ionization cross sections for collisions of  $A^{+q} + H$  in the velocity range of  $(2-7) \times 10^8$  cm/sec. The calculations employ a three-dimensional Monte Carlo approach that uses a classical description of the H atom and the Coulomb forces among all particles to obtain the cross sections. The positive ions studied include fully stripped  $A^{+q}$ , with  $q = 1-8, 10, 14, 18, 26,$  and  $36$ , and partially stripped  $B^{+q}, C^{+q}, N^{+q},$  and  $O^{+q}$ , with  $q \geq 3$ . The total electron-loss cross sections (sum of charge exchange and impact ionization) vary only slightly with velocity for the higher charge states and reach a value of  $2 \times 10^{-14}$  cm<sup>2</sup> for  $Kr^{+36} + H$  collisions. The importance of impact ionization relative to charge transfer is found to decrease with increasing  $q$  in the velocity range studied. Transition probabilities versus impact parameters are presented for the  $H^+ + H$  and  $Ar^{+18} + H$  reactions. The calculations are in reasonable agreement with experimentally measured cross sections for the  $H^+, C^{+q}, N^{+q},$  and  $O^{+q} + H$  systems.

### I. INTRODUCTION

Inelastic collision processes involving multi-charged ions and H atoms are of considerable interest, not only theoretically but also in connection with practical aspects of controlled thermonuclear fusion development. Thus, one of the most promising methods of heating and fueling a Tokamak fusion plasma is by injection of energetic H or D atoms in the velocity range of  $(3-5) \times 10^8$  cm/sec. However, a serious problem in this method arises because of the small percentage [(1-10)%] of highly stripped impurity ions<sup>1</sup> such as C, N, O, Si, Fe, Mo, or W contained in the plasma. When the injected H or D atom collides with one of these impurity ions, it is highly probable that the injected particle will lose its electron either by charge exchange or impact ionization. If this occurs on the outer edge of the plasma, the ionized H or D atom is magnetically deflected out of the plasma to strike the container walls. As a result, more impurity atoms are sputtered off the walls and enter the plasma region, with the result that it becomes increasingly difficult to heat the plasma.<sup>2</sup>

In this paper, we address the problem of calculating the electron-loss cross sections in the velocity range from  $2 \times 10^8$  to  $6 \times 10^8$  cm/sec for the reactions



Past theoretical work on these problems have been confined mainly to the  $H^+ - H$  and  $He^{+2} - H$  systems with only a limited attention paid to the heavier ion collisions.<sup>3,4</sup> Most of the quantum-theory

calculations of ionization have been in various versions of the Born approximation,<sup>5-7</sup> although some recent studies have applied higher-order theories such as the Glauber approach.<sup>8</sup> The charge-transfer process<sup>9</sup> has received a great deal of attention with a variety of techniques being utilized such as the Oppenheimer-Brinkman-Kramers<sup>10,11</sup> and Born approximations,<sup>12,13</sup> and coupled-state theories involving both atomic<sup>14-18</sup> and molecular<sup>19</sup> basis set expansions. Classical approaches such as the binary encounter theory<sup>20-22</sup> and the classical trajectory Monte Carlo approach<sup>23,24</sup> have also been applied in these problems with success, particularly in the latter case, comparable to that of the quantum calculations.

In the present study, the classical trajectory method was used in the calculation of the stripped-ion cross sections. The method was chosen for a variety of reasons. Abrines and Percival<sup>23,24</sup> had obtained good results with it for  $H^+ - H$  scattering. It has the advantage of giving both the ionization and electron-capture cross sections consistently in the same calculation. Quantum theories are particularly difficult to apply in the region of collision velocities comparable to the orbital electron velocities of the target atom. Finally, perturbation theories such as lower-order Born approximations are not really appropriate where strong interactions are involved such as in the case of a heavy multicharged ion colliding with a light, low- $Z$  target.

The results obtained in the present study indicate that these stripped-ion cross sections do not have the simple  $q^2$  scaling property one might expect on the basis of high-energy theories such as the binary encounter approximation,<sup>20-22</sup> and it seems clear that one cannot hope to obtain cross sections

for the heavier stripped ions at these collision energies by a simple scaling of the  $H^+ + H$  values.

Few experimental data exist for fully stripped  $A^{+q}$  ions, except for the<sup>25-31</sup>  $H^+ + H$  and<sup>32,33</sup>  $He^{++} + H$  reactions, although measurements are being planned for reactions of low- $Z$  ions such as  $B^{+5}$ .<sup>34</sup> However, data are now becoming available<sup>35</sup> for partially stripped ions such as  $C^{+q}$ ,  $N^{+q}$ , and  $O^{+q}$ .

In Secs. II-IV, we present the theoretical description of the problem, followed by the cross-section calculations for stripped positive ions and partially stripped positive ions.

## II. THEORY

By averaging over many appropriately chosen three-dimensional trajectories, the Monte Carlo method has been successfully used to estimate the cross sections for chemical reactions. Pioneering work began with the study of the  $H + H_2$  reaction by Hirschfelder *et al.*<sup>36</sup> four decades ago. However, because the classical trajectories had to be calculated by hand, only one trajectory was undertaken in this early study. Since the advent of the computers, the classical trajectory method has become an extremely powerful technique for calculating cross sections for chemical reactions<sup>37</sup> and has been used quite successfully for calculating the charge exchange and ionization cross sections for the  $H^+ + H$  system.<sup>23,24</sup> We outline the approach used here in which the formulation is in terms of appropriate center-of-mass coordinates<sup>38</sup> rather than the relative coordinates used by Abrines and Percival.<sup>23,24</sup>

Hamilton's equations of motion for a three-body system (12 coupled equations) are numerically solved for numerous trajectories. The impact parameter of projectile  $A$  colliding with target  $BC$ , and the orientation and momentum of  $C$  moving about  $B$  are randomly selected by the Monte Carlo method. For this discussion of reaction (1a) and (1b),  $A$  represents the  $A^{+q}$  positive ion,  $B$  the  $H$  atom nucleus, and  $C$  the electron initially moving about the hydrogen nucleus. The forces between the three bodies are taken to be Coulombic, which is exact for the case of a fully stripped  $A^{+q}$  ion.

Individual trajectories for the  $A + BC$  reaction are evaluated by placing  $A$  a large distance from  $BC$  and integrating the equations of motion until  $A$  is a large distance from  $B$ . If at the end of the collision  $C$  is still in an orbit around  $B$ , then there was no reaction. However, if  $C$  is found bound to  $A$ , charge transfer occurred and is appropriately tabulated in the computer program. If  $C$  is found not bound to either  $A$  or  $B$ , then ionization occurred during the collision. To estimate the cross sections for charge transfer and impact ionization,

it is normally necessary to calculate 1000 to 2000 trajectories to reduce the statistical error to a reasonable level.

Because Karplus *et al.*<sup>38</sup> present the classical trajectory method in detail, we will discuss only the formulation of the method that is pertinent to determining the cross sections for reactions (1a) and (1b). We simplify this presentation by employing the generalized coordinate  $C_j$  ( $j=1, 2, \dots, 9$ ), where  $C_1, C_2, C_3$  represent the Cartesian coordinates of particle  $C$  (the electron) with respect to  $B$  ( $H$  atom nucleus).  $C_4, C_5, C_6$  are the Cartesian coordinates of particle  $A$  (the  $A^{+q}$  ion) with respect to the center of mass of the  $BC$  pair, and  $C_7, C_8, C_9$  are the Cartesian coordinates of the center of mass of the entire three-body system. Likewise,  $P_j$  ( $j=1, 2, \dots, 9$ ) represent the momenta that are coupled to the  $C_j$  coordinates.

Hamilton's equations of motion are then given by the 12 coupled equations

$$\begin{aligned} \dot{C}_j &= \left( \frac{1}{m_B} + \frac{1}{m_C} \right) P_j \quad (j=1, 2, 3), \\ \dot{C}_j &= \left( \frac{1}{m_A} + \frac{1}{m_B + m_C} \right) P_j \quad (j=4, 5, 6), \\ \dot{P}_j &= \frac{m_C}{m_B + m_C} \left( \frac{m_C}{m_B + m_C} C_j + C_{j+3} \right) \left( \frac{Z_A Z_C}{R_1^3} \right) + C_j \left( \frac{Z_B Z_C}{R_2^3} \right) \\ &\quad + \frac{m_B}{m_B + m_C} \left( \frac{m_B}{m_B + m_C} C_j - C_{j+3} \right) \left( \frac{Z_A Z_C}{R_3^3} \right) \quad (j=1, 2, 3), \\ \dot{P}_j &= \left( \frac{m_C}{m_B + m_C} C_{j-3} + C_j \right) \left( \frac{Z_A Z_B}{R_1^3} \right) \\ &\quad - \left( \frac{m_B}{m_B + m_C} C_{j-3} - C_j \right) \left( \frac{Z_A Z_C}{R_3^3} \right) \quad (j=4, 5, 6). \end{aligned} \quad (2)$$

The terms containing the center of mass of the three-body system,  $j=7-9$ , have been subtracted from Eqs. (2) because they are constants of motion. In Eqs. (2),  $Z_A, Z_B$ , and  $Z_C$  are the charges of the three particles; for our purposes,  $Z_A = q$ ,  $Z_B = +1.0$ , and  $Z_C = -1.0$ . The internuclear separation  $R_1$  is taken between  $A$  and  $B$ ,  $R_2$  between  $B$  and  $C$ , and  $R_3$  between  $A$  and  $C$ . The internuclear separations are evaluated in terms of the Cartesian coordinates  $C_j$  to yield

$$\begin{aligned} R_1 &= \left[ \left( \frac{m_C}{m_B + m_C} C_1 + C_4 \right)^2 + \left( \frac{m_C}{m_B + m_C} C_2 + C_5 \right)^2 \right. \\ &\quad \left. + \left( \frac{m_C}{m_B + m_C} C_3 + C_6 \right)^2 \right]^{1/2}, \\ R_2 &= (C_1^2 + C_2^2 + C_3^2)^{1/2}, \end{aligned} \quad (3)$$

and

$$\begin{aligned} R_3 &= \left[ \left( \frac{m_B}{m_B + m_C} C_1 - C_4 \right)^2 + \left( \frac{m_B}{m_B + m_C} C_2 - C_5 \right)^2 \right. \\ &\quad \left. + \left( \frac{m_B}{m_B + m_C} C_3 - C_6 \right)^2 \right]^{1/2}. \end{aligned}$$

To begin the numerical integration of Eqs. (2), initial values of the  $C_j$  and  $P_j$  must be defined. If the  $z$  axis is chosen as the direction of the initial relative velocity vector, then

$$P_4^0 = P_5^0 = 0 \quad (4)$$

and

$$P_6^0 = \left( \frac{1}{m_A} + \frac{1}{m_B + m_C} \right) v_{\text{rel}}$$

Furthermore, if the coordinate system is oriented so that  $A$  and the center of mass of  $BC$  lie in the  $y$ - $z$  plane, then

$$C_4^0 = 0, \quad C_5^0 = b, \quad (5)$$

and

$$C_6^0 = -(R_*^2 - b^2)^{1/2},$$

where  $b$  is the impact parameter and  $R_*$  is the initial distance of  $A$  from the center of mass of  $BC$ . For the case at hand,  $R_*$  was normally set equal to  $10q$  Bohr radii.

The initial coordinates for particle  $C$ , with  $B$  as the origin (the electron orbiting about the H atom nucleus), are given in terms of the spherical polar coordinates  $R_e$ ,  $\theta$ , and  $\varphi$ :

$$\begin{aligned} C_1^0 &= R_e \sin\theta \cos\varphi, \\ C_2^0 &= R_e \sin\theta \sin\varphi, \quad \text{and} \quad C_3^0 = R_e \cos\theta. \end{aligned} \quad (6)$$

In Eq. (6),  $R_e$  is the distance between  $B$  and  $C$ , and  $\theta$  and  $\varphi$  are determined by the Monte Carlo method. The initial components of the momenta of  $C$  relative to  $B$  are given in terms of  $P_e$ , the magnitude of the momentum of  $C$  with respect to  $B$ , and an additional angle  $\eta$  that is selected randomly in the Monte Carlo method:

$$\begin{aligned} P_1^0 &= -P_e (\sin\varphi \cos\eta + \cos\varphi \cos\theta \sin\eta), \\ P_2^0 &= P_e (\cos\varphi \cos\eta - \sin\varphi \cos\theta \sin\eta), \\ P_3^0 &= P_e \sin\theta \sin\eta. \end{aligned} \quad (7)$$

A difficulty arises in determining  $R_e$  and  $P_e$  to accurately represent  $BC$ , which for our purposes is the H atom. Fortunately, Abrines and Percival<sup>23,24</sup> have carefully formulated a classical description for the H atom. They argue that the spherically symmetric hydrogen atom ground state can be represented by a microcanonical ensemble. The method requires, for each randomly selected orbit, an iterative solution of Kepler's equation

$$\theta_n = u - \epsilon \sin u, \quad (8)$$

where  $u$  is the eccentric angle and  $\epsilon$  is the eccentricity of the orbit. The angle  $\theta_n$ , along with  $\epsilon$ , is determined by the Monte Carlo method. Given  $\theta_n$  and  $\epsilon$ , an iterative solution is required to define

the angle  $u$ .

Once  $\epsilon$  and  $u$  are defined, it is then possible to calculate  $R_e$  and  $P_e$ . For a hydrogenic atom or ion target

$$R_e = (Z/2U)(1 - \epsilon \cos u)$$

and

$$P_e = (2U)^{1/2} (1 - \epsilon^2 \cos^2 u)^{1/2} / (1 - \epsilon \cos u), \quad (9)$$

where  $U$  is the binding energy in atomic units of the electron on the target atom or ion.

Given Eqs. (2)–(9), we need only choose six pseudorandom numbers, and the initial positions and velocities before numerically integrating the classical trajectory. The six parameters, which are varied for each trajectory, are given in the following along with their limits:

$$-\pi \leq \varphi \leq \pi; \quad -1 \leq \cos\theta \leq 1; \quad -\pi \leq \eta \leq \pi; \quad (10)$$

$$0 \leq \epsilon^2 \leq 1; \quad 0 \leq \theta_n \leq 2\pi; \quad 0 \leq b^2 \leq b_{\text{max}}^2.$$

In Eq. (10),  $b_{\text{max}}$  is the largest value of the impact parameter for which charge transfer or impact ionization can occur. With experience, one can choose an appropriate  $b_{\text{max}}$  for a given system quite rapidly; initially, however, one must repeat the calculations to obtain the best value. If  $b_{\text{max}}$  is given too large a value, an excessive number of trajectories must be calculated before the statistical error on the cross sections reduces to a reasonable level.

After each trajectory has been integrated (we employed the Runge-Kutta-Gill method with variable step size) to the distance of closest approach and then out to at least a distance between  $A$  and  $B$  of  $10q$  ( $a_0$ ), it is necessary to check for reaction. If particle  $C$  is still bound to  $B$ , then no reaction has occurred. However, if  $C$  is found bound to particle  $A$ , it is counted as charge transfer. If  $C$  is found receding from both  $A$  and  $B$ , it is counted as impact ionization. A problem arises, however, with a limited number of trajectories for which  $C$ , the electron, is left dangling between  $A$  and  $B$ . One must then be careful to integrate to much larger internuclear separations to make sure that  $C$  is not subsequently captured by either particle  $A$  (charge transfer) or particle  $B$  (no reaction). For these few trajectories, it is not unusual to integrate until the  $A$ - $B$  internuclear separation is  $1000 q(a_0)$ .

Once a significant number of trajectories have been calculated (usually on the order of 1000–2000), it is possible to calculate the cross sections by

$$Q_R = (N_R/N) \pi b_{\text{max}}^2. \quad (11)$$

In Eq. (11), the cross section for reaction  $Q_R$  ( $R$  may represent charge transfer, ionization, or the sum of the two) is proportional to the number of

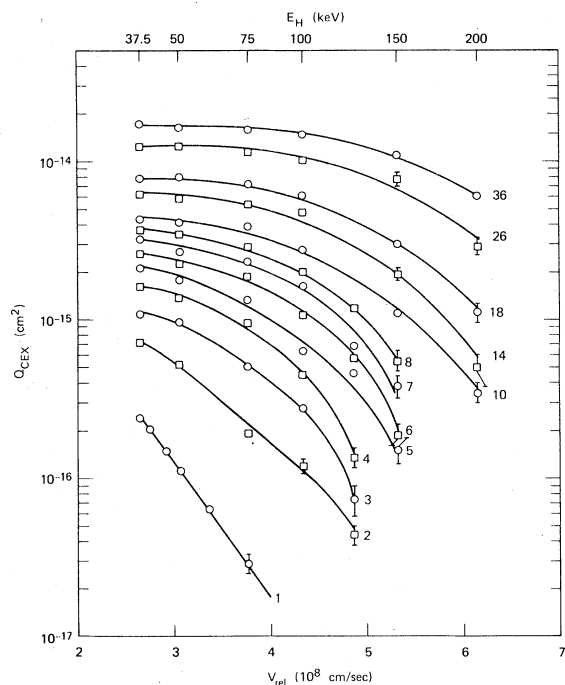


FIG. 1. Calculated charge exchange total cross sections for fully stripped  $A^{+q}$  ions colliding with H atoms. The indexing numbers refer to the  $Z=q$  of the  $A^{+q}$  ions. Points with error bars have statistical errors greater than 10% and should be viewed with caution.

collisions satisfying the criteria for reaction  $N_R$  divided by the total number of trajectories calculated  $N$ . Likewise, the standard deviation for the reactive cross section is given by

$$\Delta Q_R = Q_R [(N - N_R)/NN_R]^{1/2}. \quad (12)$$

We emphasize that the classical trajectory method incorporates all the forces between the three bodies; hence, the deflection of the particles is included in the calculations. Curvilinear trajectories are important for more accurately representing the collisions of highly charged  $A^{+q}$  ions that collide with H atoms because the strong Coulomb force can significantly distort the reactive trajectories for low-keV-energy collisions.

### III. CROSS SECTIONS

#### A. Fully stripped $A^{+q}$ ions

Equations (2)–(12) have been programmed and used to calculate the charge exchange and impact ionization cross sections for a wide range of fully stripped positive ions ( $H^+$  to  $Kr^{+36}$ ) colliding with H atoms. Each cross section determination took approximately  $0.1q$  min of CDC 7600 computing time. Note that the charge exchange cross section corresponds to a capture into any of the bound states of

the ion; that is, a total capture cross section rather than a capture into the ground state only. The collision energy range covered was from an equivalent H atom energy  $E_H$  of 37.5 to 200 keV. (At lower collision energies, molecular processes become important and the classical method is inappropriate. The calculations were not made at higher energies because the transition probabilities become small; in addition, quantum-mechanical effects, which are not incorporated in our present theoretical treatment, would negate the validity of the classical cross sections.)

The results of the classical trajectory calculations for the charge exchange cross sections  $Q_{CEX}$ , impact ionization cross sections  $Q_{ION}$ , and the sum of the charge exchange and ionization cross section  $Q_{LOSS}$  are presented in Figs. 1–3. We include the  $Q_{LOSS}$  values because the statistical errors for this cross section are smaller than either of its components; hence, the cross sections should be more reliable.

The charge exchange cross sections, Fig. 1, show a progressively weaker energy dependence as the  $q=Z$  of the stripped projectile increases from  $H^+$  or  $Kr^{+36}$ . In fact, in the velocity range studied, the high- $Z$  projectiles possess almost constant cross sections over a wide range of velocities. At lower energies, they seem to approach the values given by an absorbing-sphere method,<sup>39</sup> which is applicable for low-keV-energy collisions. Note that a simple  $Z^2$  scaling of the  $H^+ + H$  cross

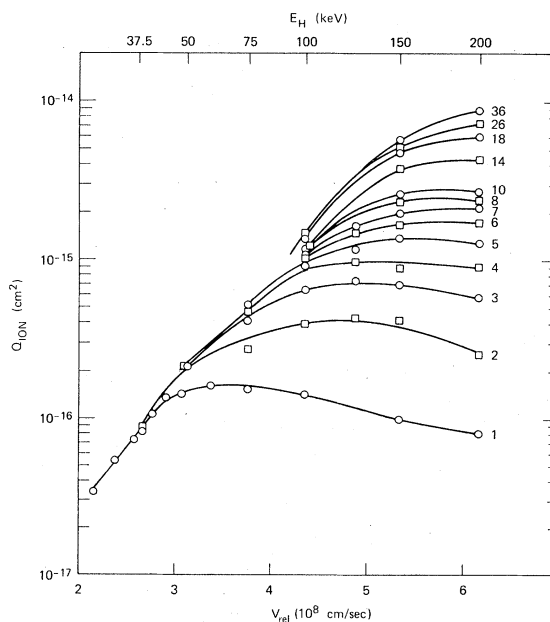


FIG. 2. Calculated impact ionization total cross sections for fully stripped  $A^{+q}$  ions colliding with H atoms. The indexing numbers refer to the  $Z=q$  of the  $A^{+q}$  ions.

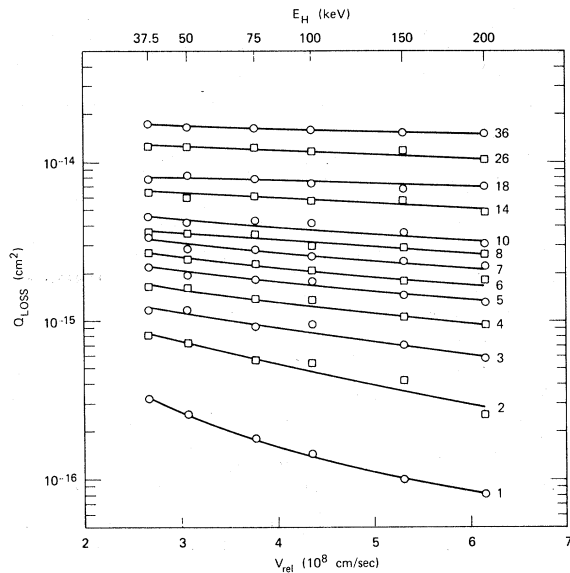


FIG. 3. Calculated total cross sections for electron loss (sum of charge exchange and impact ionization) from H atoms by collisions with fully stripped  $A^{+q}$  ions. The indexing numbers refer to the  $Z=q$  of the  $A^{+q}$  ions.

section would not reproduce the magnitude or the shape of the cross sections presented here. The cross sections that are shown with error bars have statistical errors in excess of 10% and should be viewed with caution.

The impact ionization cross sections in Fig. 2 have very different energy dependences from that predicted by the binary encounter approximation<sup>21</sup> for which the cross sections scale as  $Z^2$  times the  $H^+ + H$  results. These ionization cross sections peak at higher and higher velocities as  $Z$  increases because any electron removed from the H atom is preferentially captured by the strong Coulomb field of the projectile. This results in charge transfer, not ionization. Our calculations also show that the ionization cross sections for all  $Z$  have the same exponential velocity dependence in the threshold energy region.

The sum of the charge exchange and impact ionization cross sections  $Q_{LOSS}$  are presented in Fig. 3. These cross sections are almost constant in velocity for the higher- $Z$  values. At a collision energy of  $E_H = 50$  keV, the cross sections scale approximately as  $2.5 \times 10^{-16} Z^{5/4} (\text{cm}^2)$ .

Our cross sections for  $H^+ + H$  are in agreement with the Monte Carlo results of Abrines and Percival and the more recent work of Banks *et al.*,<sup>40</sup> and were in fact used to check our computer code. The earlier calculations had been shown to be in reasonable agreement with the available experimental data, and this was a strong motivation for carrying out the present study. Indeed, to date,

$H^+ + H$  is still the only relevant stripped-ion collision system for which comprehensive experimental data exist in the velocity range of interest. The  $H^+ + H$  results are of special importance in these calculations because they serve as a frame of reference in which to view the entire set of stripped ion-hydrogen calculations. We therefore present in Figs. 4 and 5, plots of the computed charge transfer and ionization  $H^+ + H$  cross sections and comparisons with other available results notwithstanding the similarities to the data previously given by Abrines and Percival.<sup>23,24</sup>

In Fig. 4, the classical trajectory calculations for charge exchange (denoted by the solid line) are compared with the experimental values of McClure<sup>28</sup> (open circles). The agreement is good, except at the lowest and the highest energies where the theoretical values underestimate the experimental results. Other experimental studies give similar good agreement.<sup>27,29,30</sup> At collision velocities comparable to the orbital velocity of the electron on the H target ( $v = 2.2 \times 10^8$  cm/sec,  $E_H = 25$  keV), molecular processes become important; as a result, we can expect the classical trajectory calculations to give only a rough estimate of the cross section. At the highest collision energies, the probability for charge transfer becomes very small, and it is necessary to run several hundred trajectories before obtaining a positive test for charge transfer. Hence, not only are the statistical errors larger, but we must also be concerned that our pseudorandom number generator used for

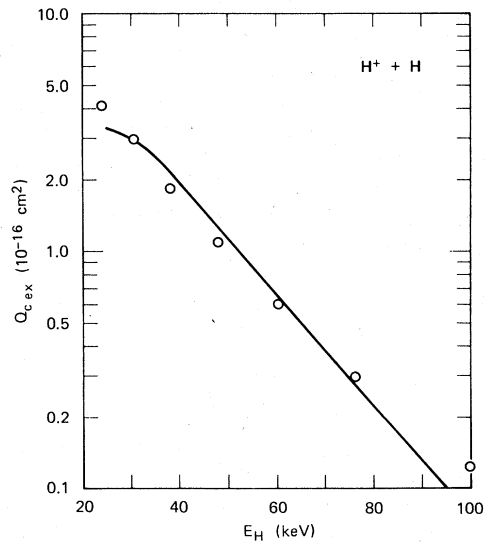


FIG. 4. Classical trajectory calculations for the charge exchange cross sections for collisions of  $H^+ + H$  (solid line) versus the experimental data of McClure, Ref. 28 (open circles).

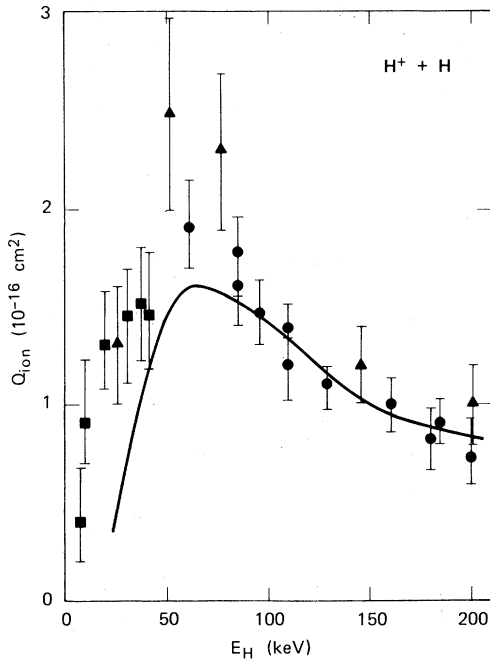


FIG. 5. Classical trajectory calculations for the impact ionization cross sections for collisions of  $H^+ + H$  (solid line) versus the experimental data of: Fite *et al.*, Ref. 29 (solid squares); Gilbody and Ireland, Ref. 26 (solid circles); and Park *et al.*, Ref. 31 (solid triangles).

the initial conditions is not truly random and thus biases the results. A further complication is that we are not allowing for quantum tunneling in the description of the electron about the H nucleus; this tunneling may be important when the transition probabilities become small. Given these problems, it is not surprising that our results are not in good agreement with experiments at the highest energy shown in Fig. 4.

In Fig. 5, various experimental  $H^+ + H$  impact ionization cross sections<sup>26,29,31</sup> are compared with the present Monte Carlo results. At energies  $E_H$  above  $\sim 75$  keV, theory and experiment are in good agreement. However, at the lower energies, the classical trajectory values tend to greatly underestimate the experimental cross sections.

By extrapolating the Monte Carlo charge-transfer values for the  $He^{++} + H$  systems to slightly lower energies, we can compare our results with experimental measurements. The results are in reasonable agreement ( $\sim 20\%$  low) with the measurements of Shah and Gilbody<sup>32</sup> but are almost a factor of 2 below the values of Bayfield and Khayrallah.<sup>33</sup> Hence, a conclusive test of the classical calculations on the  $He^{++} + H$  system is impossible until this experimental discrepancy is removed.

To more clearly demonstrate the differences between low- $Z$  and high- $Z$  projectile collisions with

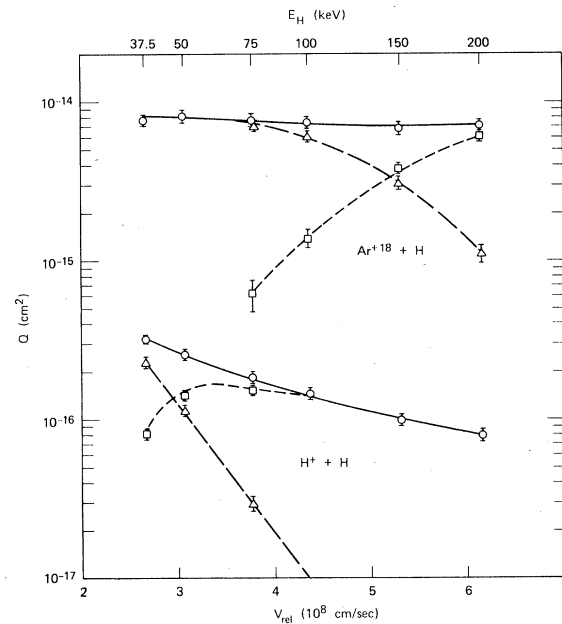


FIG. 6. Calculated cross sections for  $H^+ + H$  and  $Ar^{+18} + H$  collisions. The charge transfer cross sections are denoted by open triangles, the impact ionization cross sections by open squares, and the total H electron-loss cross sections by open circles.

$H$ , we present, in Fig. 6, the cross sections for  $H^+ + H$  and  $Ar^{+18} + H$ . It is apparent that, as the  $Z$  of the projectile increases, charge transfer dominates impact ionization as the principal mechanism of electron loss from the H target to higher collision velocities.

We also present the impact parameter dependence of the transition probabilities for charge exchange and impact ionization for a limited number of selected systems. For this study, we have again chosen the  $H^+ + H$  and  $Ar^{+18} + H$  systems. The calculated values for  $H^+ + H$  for a series of collision energies are shown in Figs. 7 and 8, and values

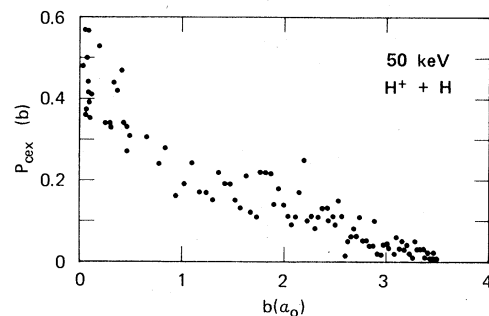


FIG. 7. Transition probabilities vs impact parameter for charge exchange in  $E_H = 50$ -keV collisions of  $H^+ + H$ . Each point represents the result of 100 classical trajectories.

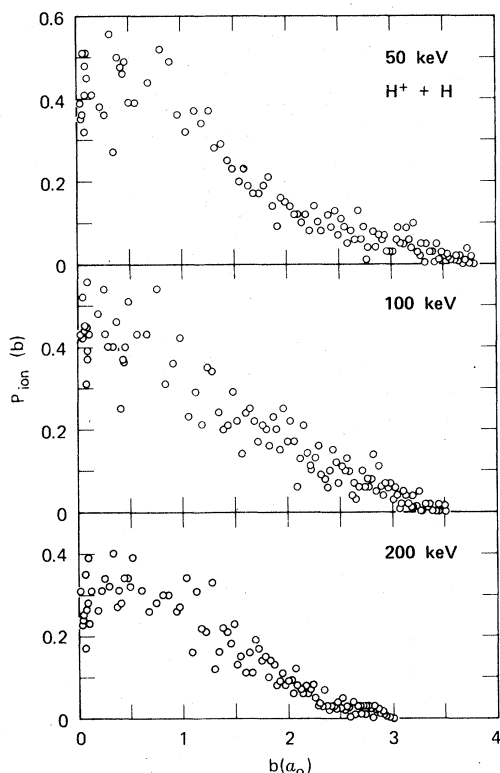


FIG. 8. Transition probabilities for impact ionization in  $E_H = 50$ -,  $100$ -, and  $200$ -keV collisions of  $H^+ + H$ . Each circle represents the result of 100 classical trajectories.

for  $Ar^{+18} + H$  are given on Figs. 9 and 10. Each point on the figures represents the result of 100 trajectory calculations. For the  $H^+ + H$  system in Figs. 7 and 8, all transition probabilities have a maximum at the zero impact parameter and then decrease monotonically to zero at  $b \approx (3-4)a_0$ . The range of the coupling also decreases slightly as the collision energy increases.

Probably more interesting are the results of the  $Ar^{+18} + H$  calculations, Figs. 9 and 10. Charge transfer in Fig. 9 is found to proceed with almost unit probability for the small impact parameter collisions at  $E_H = 50$  and  $100$  keV; unexpectedly, the ionization transition probabilities in Fig. 10 at  $100$  keV display a maximum at  $b \approx 10a_0$ . This behavior occurs because, for small impact parameter collisions at the lower collision energies, the electron initially orbiting about the  $H$  nucleus is strongly attracted by the  $-18/R$  Coulomb potential to the  $Ar^{+18}$  ion, thus charge transfer occurs. Not until the collision proceeds with higher velocity or a large impact parameter collision occurs, can the electron escape the Coulomb fields of the two nuclei to ionize into the continuum.

We have also investigated the possibility of isotope effects on the cross sections. For collisions of  $A^{+q} + H$  vs  $A^{+q} + D$ , we could discern no observable change in the cross sections for  $q \geq 2$  as a function of relative velocity.

#### B. Partially stripped $A^{+q}$ ions

The formulation of the classical trajectory method assumes we are dealing with a three-body problem. However, a considerable amount of interest lies in the prediction of the cross sections for partially stripped  $A^{+q}$  ions colliding with  $H$ . It is ex-

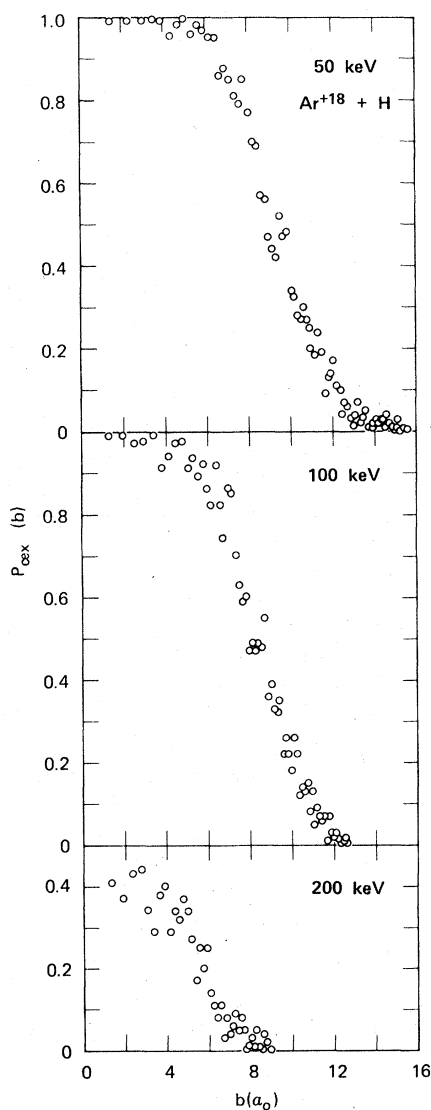


FIG. 9. Transition probabilities for charge exchange in  $E_H = 50$ -,  $100$ -, and  $200$ -keV collisions of  $Ar^{+18} + H$ . Each circle represents the result of 100 classical trajectories.

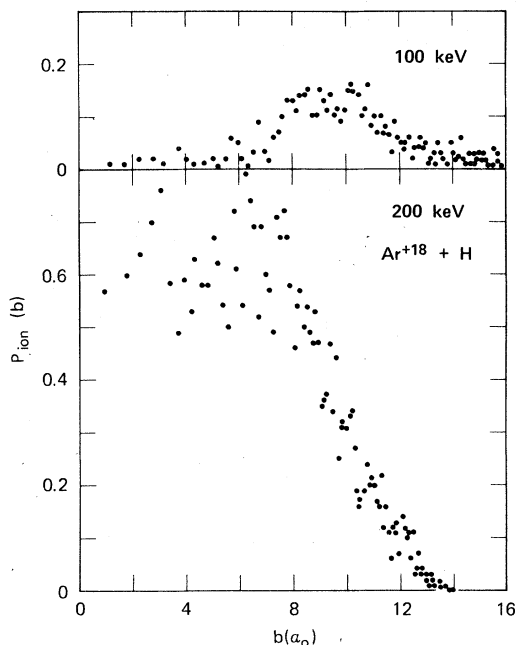


FIG. 10. Transition probabilities for impact ionization in  $E_H = 100$ - and  $200$ -keV collision of  $\text{Ar}^{+18} + \text{H}$ . Each point represents the result of 100 classical trajectories.

perimentally difficult to strip heavy atoms of all their electrons for experiments in the low-keV-energy range. Moreover, experimental data are now becoming available<sup>35,41</sup> for partially stripped systems such as  $\text{C}^{+q}$ ,  $\text{N}^{+q}$ ,  $\text{O}^{+q}$ , and  $\text{Fe}^{+q}$ . Therefore, we have attempted to modify the classical method to address this problem.

From the results of our calculations for fully stripped ions, we can argue that the dominant region of interaction between  $A^{+q}$  and H is at internuclear separations that are comparable to the mean radii of excited electronic levels of the  $A^{+q}$  ion. Hence, we must determine the effective charge  $q_{\text{eff}}$  of the ion as felt by an electron captured in one of the ion's excited states whose radius is approximately the same as the impact parameters that predominately determine the cross sections. Because of correlation effects between the excited state electron and the core electrons, the effective charge of the ion will normally be less than its asymptotic value.

An effective potential method of the Hellman type<sup>42</sup> can be used to determine the  $R$  dependence of  $q_{\text{eff}}$ . However, as an alternative approach, we have assumed that the  $A^{+q-1}$  ion can be reasonably approximated by a hydrogenic model and have used spectroscopic energy level data to determine  $q_{\text{eff}}$ . The principal quantum numbers of the excited electronic levels were reordered in the same manner as employed in the effective potential approach of

Simons<sup>43</sup> so that the ground state corresponds to  $n=1$ , the first excited level of a higher  $n$  value to  $n=2$ , etc. The ionization energies (in atomic units) were then set equal to  $q_{\text{eff}}^2/(2n^2)$  to determine  $q_{\text{eff}}$ . The value of  $q_{\text{eff}}$  obtained for the excited level  $\sim 13.6$  eV below the ionization limit was then used in the classical trajectory calculations. Such a choice assumes zero energy exchange during a charge-transfer collision. (Other reasonable choices of the excited-state level did not appreciably change  $q_{\text{eff}}$ .) By determining  $q_{\text{eff}}$  with this procedure, it was unnecessary to modify the computer program used in the fully stripped-ion cases. Rather, we only needed to set  $Z_A = q_{\text{eff}}$ .

We have used this method to calculate the cross sections for  $\text{B}^{+q}$ ,  $\text{C}^{+q}$ ,  $\text{N}^{+q}$ , and  $\text{O}^{+q} + \text{H}$ , when  $q \geq 3$ . The calculated cross sections are presented in Figs. 11–14, and the  $q_{\text{eff}}$  values used in the com-

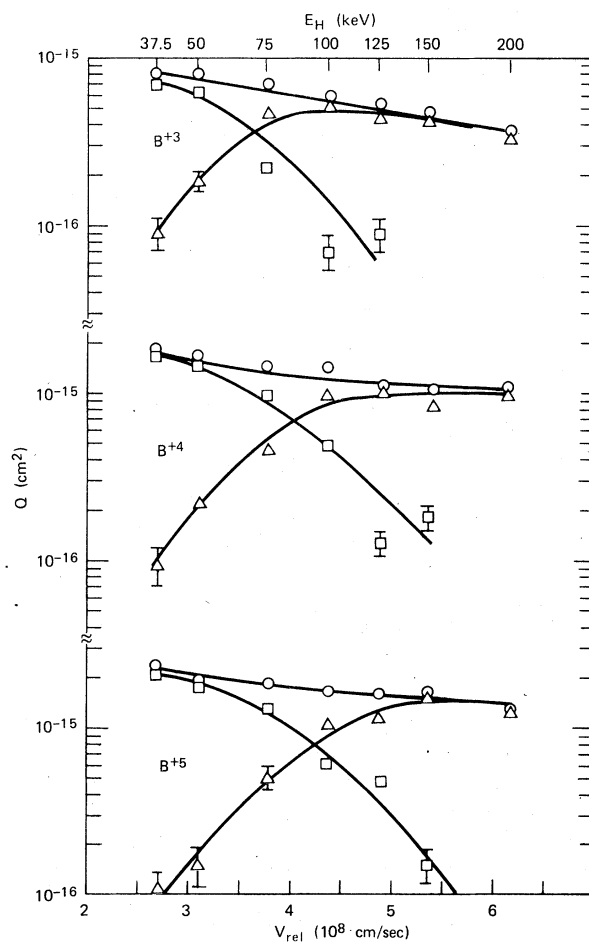


FIG. 11. Calculated cross sections for  $\text{B}^{+q} (q=3-5) + \text{H}$  collisions. The open squares denote the charge-transfer cross sections, the open triangles the impact ionization cross sections, and the open circles the total cross sections for electron loss by the H atom.



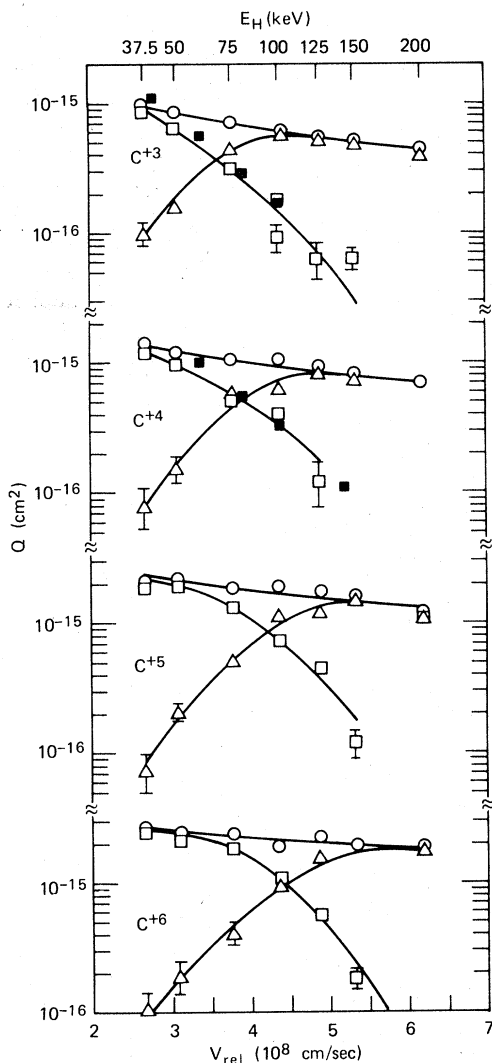


FIG. 12. Cross sections for  $C^{+q}$  ( $q=3-6$ ) + H collisions. The open squares denote the theoretical charge transfer cross sections that should be compared to the experimental measurements for  $q=3, 4$  by Phaneuf *et al.*, Ref. 35 (solid squares). The theoretical cross sections for impact ionization are denoted by the open triangles, and the open circles denote the total cross sections for electron loss by the H atom.

putations are given in Table I. We would also have liked to calculate the cross sections for  $Fe^{+q}$  to compare with the recently available experimental data.<sup>41</sup> However, insufficient spectroscopic data were available on the excited states of  $Fe^{+q}$  to determine  $q_{\text{eff}}$ .

Although no experimental data now exist on the  $B^{+q}$  systems, charge transfer (capture of the H electron by the positive ion) cross sections have been measured by Phaneuf *et al.*<sup>35</sup> for some of the  $C^{+q}$ ,  $N^{+q}$ , and  $O^{+q}$  systems. The experimental val-

TABLE I. Effective charge  $q_{\text{eff}}$  used in the  $B^{+q}$ ,  $C^{+q}$ ,  $N^{+q}$ , and  $O^{+q}$  + H calculations.

$q$	$B^{+q}$	$C^{+q}$	$N^{+q}$	$O^{+q}$
3	2.2	2.4	2.5	2.6
4	4.0	3.2	3.2	3.4
5	5.0	5.0	4.1	4.3
6	...	6.0	6.0	5.1
7	...	...	7.0	7.0
8	...	...	...	8.0

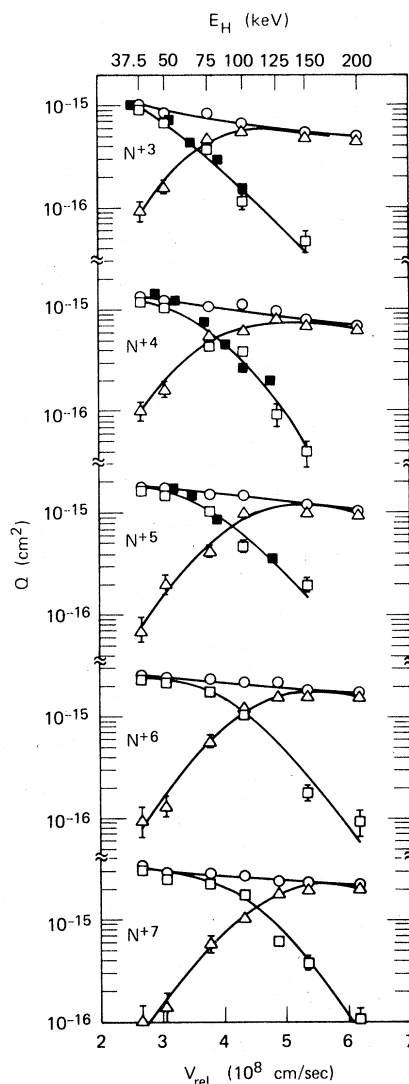


FIG. 13. Cross sections for  $N^{+q}$  ( $q=3-7$ ) + H collisions. The open squares denote the theoretical charge transfer cross sections that should be compared to the experimental measurements for  $q=3-5$  by Phaneuf *et al.*, Ref. 35 (solid squares). The theoretical cross sections for impact ionization are denoted by the open triangles, and the open circles denote the total cross sections for electron loss by the H atom.

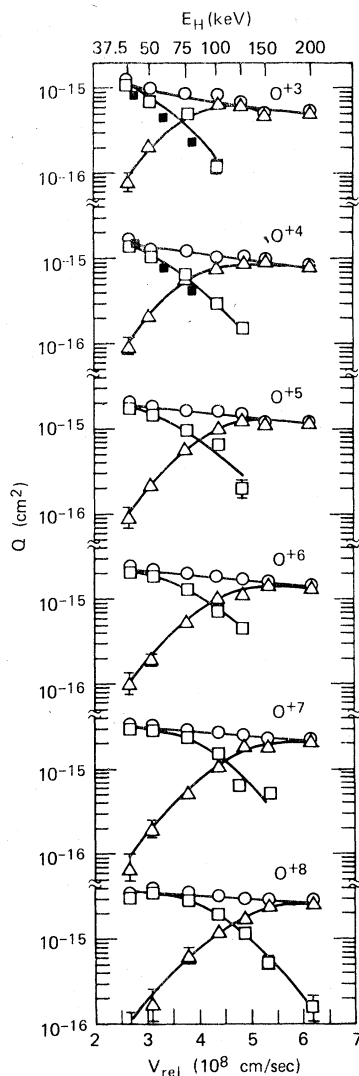


FIG. 14. Cross sections for  $O^{+q}$  ( $q=3-8$ ) + H collisions. The open squares denote the theoretical charge-transfer cross sections that should be compared to the experimental measurements for  $q=3, 4$  by Phaneuf *et al.*, Ref. 35 (solid squares). The theoretical cross sections for impact ionization are denoted by the open triangles, and the open circles denote the total cross sections for electron loss by the H atom.

ues are given by the solid squares in Figs. 12–14 and should be compared to the calculated values denoted by open squares. The agreement between theory and experiment is quite good and thus provides support for the classical trajectory approach in these types of collisions. The use of a simple  $q_{\text{eff}}$  appears to be partially justified even for the  $O^{+3}$  system that has an open  $2p$  shell which interacts strongly with the H atom electron during the col-

lision. We have also calculated the impact ionization cross sections for these partially stripped systems and anticipate these values will be tested by experimental measurements within a year.<sup>34</sup>

#### IV. SUMMARY

We have employed the classical trajectory method to calculate the charge transfer and impact ionization cross sections for a wide range of fully and partially stripped positive ions colliding with an H atom. The calculated charge-transfer cross sections are in reasonable agreement with several measured values. However, as seen in the  $H^+ + H$  calculations, these values may underestimate the “true” cross sections at the lowest energies ( $E_H \lesssim 50$  keV). A complete test of the calculated ionization cross sections is not now available, but from the  $H^+ + H$  case there is some indication that the theoretical values may also underestimate the true results at the lowest energies. At the highest energy studied in this investigation (200 keV), the theoretical ionization cross sections are in good agreement with the only system studied experimentally,  $H^+ + H$ .

The calculations also indicate the competition between charge transfer and impact ionization processes as the charge of the  $A^{+q}$  ion is varied. They predict that charge transfer will dominate the electron removal from H at higher velocities as the charge  $q$  is increased. In addition, the impact ionization cross sections tend to exhibit the same exponential growth in the threshold energy region for all values of  $q$  and to peak at higher velocities as  $q$  increases.

We have also addressed the problem of calculating the cross sections for partially stripped  $A^{+q}$  ions colliding with H. A simple method has been devised to use an effective charge  $q_{\text{eff}}$  for the  $A^{+q}$  ion, which is appropriate to the internuclear separation range that determines the cross sections. Comparison with experimental data indicates that this approach is reasonable.

The cross sections calculated here indicate that no simple  $q^2$  scaling of the  $H^+ + H$  cross sections can be used to obtain the cross sections for a wide range of  $A^{+q} + H$  systems. Only in the high-velocity region where the charge transfer cross sections decrease rapidly is it possible to scale the charge-transfer cross sections as  $q^2$  for the fully stripped ions or  $q_{\text{eff}}^2$  for the partially stripped ions. At a collision velocity corresponding to  $E_H \approx 50$  keV, the sum of the charge transfer and impact ionization cross sections were found to scale roughly as  $2.5 \times 10^{-16} q^{5/4}$  ( $\text{cm}^2$ ).

- \*Work supported by ERDA Contract No. E(04-3)-115, P/A No. 111.
- <sup>1</sup>E. Hinnov, Phys. Rev. A 14, 1533 (1976).
  - <sup>2</sup>J. Hogan and H. C. Howe, Bull. Am. Phys. Soc. 20, 1228 (1975).
  - <sup>3</sup>A. Z. Msezane, Phys. Lett. A 59, 435 (1977).
  - <sup>4</sup>L. P. Presnyakov and A. D. Ulansev, Kvant. Elektron. 1, 2377 (1974) [Sov. J.-Quantum. Electron. 4, 1320 (1975)].
  - <sup>5</sup>D. R. Bates and G. W. Griffing, Proc. Phys. Soc. Lond. A 66, 961 (1953).
  - <sup>6</sup>A. Salin, J. Phys. B 2, 631 (1969).
  - <sup>7</sup>D. R. Bates and R. J. Tweed, J. Phys. B 7, 117 (1974).
  - <sup>8</sup>J. E. Golden and J. H. McGuire, J. Phys. B 9, L11 (1976).
  - <sup>9</sup>See M. R. C. McDowell and J. P. Coleman, *Introduction to the Theory of Ion-Atom Collisions* (North-Holland, Amsterdam, 1970), Chap. 8, for a discussion of the theoretical techniques used in studying charge-transfer processes.
  - <sup>10</sup>H. C. Brinkman and H. A. Kramers, Proc. Acad. Sci. Amsterdam 33, 973 (1930).
  - <sup>11</sup>J. R. Oppenheimer, Phys. Rev. 31, 349 (1928).
  - <sup>12</sup>J. D. Jackson and H. Schiff, Phys. Rev. 89, 359 (1953).
  - <sup>13</sup>K. Omidvar, Phys. Rev. A 12, 911 (1975).
  - <sup>14</sup>R. McCarroll, Proc. R. Soc. A 264, 547 (1961).
  - <sup>15</sup>R. McCarroll and M. B. McElroy, Proc. R. Soc. A 266, 422 (1962).
  - <sup>16</sup>D. Rapp, J. Chem. Phys. 58, 2043 (1973).
  - <sup>17</sup>A. Msezane and D. F. Gallaher, J. Phys. B 6, 2334 (1973).
  - <sup>18</sup>L. Wilets and D. F. Gallaher, Phys. Rev. 147, 13 (1966).
  - <sup>19</sup>R. D. Piacentini and A. Salin, J. Phys. B 7, 1666 (1974); and correction (to be published).
  - <sup>20</sup>M. Gryzinski, Phys. Rev. 115, 374 (1959).
  - <sup>21</sup>J. D. Garcia, E. Gerjuoy and J. E. Welker, Phys. Rev. 165, 66 (1968).
  - <sup>22</sup>L. Vriens, Proc. Phys. Soc. Lond. 90, 935 (1967).
  - <sup>23</sup>R. Abrines and I. C. Percival, Proc. Phys. Soc. Lond. 88, 861 (1966).
  - <sup>24</sup>R. Abrines and I. C. Percival, Proc. Phys. Soc. Lond. 88, 873 (1966).
  - <sup>25</sup>W. L. Fite, R. F. Stebbings, D. G. Hummer, and R. T. Brackman, Phys. Rev. 119, 663 (1960).
  - <sup>26</sup>H. B. Gilbody and J. V. Ireland, Proc. R. Soc. A 277, 137 (1963).
  - <sup>27</sup>H. B. Gilbody and G. Ryding, Proc. R. Soc. A 291, 438 (1966).
  - <sup>28</sup>G. W. McClure, Phys. Rev. 148, 47 (1966).
  - <sup>29</sup>W. L. Fite, A. C. H. Smith, and R. F. Stebbings, Proc. R. Soc. A 268, 527 (1962).
  - <sup>30</sup>A. B. Wittkower, G. Ryding, and H. B. Gilbody, Proc. Phys. Soc. Lond. 89, 541 (1966).
  - <sup>31</sup>J. T. Park, J. E. Aldag, J. M. George, and J. L. Peacher, Phys. Rev. A 15, 508 (1977).
  - <sup>32</sup>M. B. Shah and H. B. Gilbody, J. Phys. B 7, 636 (1974).
  - <sup>33</sup>J. E. Bayfield and G. A. Khayrallah, Phys. Rev. A 12, 869 (1975).
  - <sup>34</sup>D. H. Crandall (private communication).
  - <sup>35</sup>R. A. Phaneuf, F. W. Meyer, and R. H. McKnight, in *Atomic Data for Fusion*, edited by C. F. Barnett and W. L. Wiese, (U.S. GPO, Washington, D.C., 1976), Vol. 2, No. 5, pp. 20 and 21.
  - <sup>36</sup>J. Hirschfelder, H. Eyring, and B. Topley, J. Chem. Phys. 4, 170 (1936).
  - <sup>37</sup>D. L. Bunker, in *Methods in Computational Physics*, edited by B. Alder, S. Fernback, and M. Rotenberg (Academic, New York, 1971), Vol. 10, pp. 287-324.
  - <sup>38</sup>M. Karplus, R. N. Porter, and R. D. Sharma, J. Chem. Phys. 43, 3259 (1965).
  - <sup>39</sup>R. E. Olson and A. Salop, Phys. Rev. A 14, 579 (1976).
  - <sup>40</sup>D. Banks, K. S. Barnes, and J. McB. Wilson, J. Phys. B 9, L141 (1976).
  - <sup>41</sup>J. Bayfield, L. Gardner, H. Kim, and P. Stelson, in Ref. 35, p. 21.
  - <sup>42</sup>H. Hellmann, J. Chem. Phys. 3, 61 (1935).
  - <sup>43</sup>G. Simons, J. Chem. Phys. 55, 756 (1971).